

^{57}Fe Emission Mössbauer Study on $\text{Gd}_3\text{Ga}_5\text{O}_{12}$ implanted with dilute ^{57}Mn

P. B. Krastev¹ · H. P. Gunnlaugsson² · K. Nomura³ · V. Adoons⁴ ·
A. M. Gerami^{2,5} · K. Johnston² · M. Ncube⁶ · R. Mantovan⁷ · H. Masenda⁶ ·
Y. A. Matveyev⁸ · T. E. Mølholt² · I. Unzueta⁹ · K. Bharuth-Ram^{10,13} ·
H. Gislason¹¹ · G. Langouche¹² · D. Naidoo⁶ · S. Ólafsson¹¹ ·
the ISOLDE collaboration²

© Springer International Publishing Switzerland 2016

Abstract ^{57}Fe emission Mössbauer spectroscopy has been applied to study the lattice location and properties of Fe in gadolinium gallium garnet $\text{Gd}_3\text{Ga}_5\text{O}_{12}$ (GGG) single crystals in the temperature interval 300 – 563 K within the extremely dilute ($<10^{-4}$ at.%) regime following the implantation of ^{57}Mn ($T_{1/2} = 1.5$ min.) at ISOLDE/CERN. These results are compared with earlier Mössbauer spectroscopy study of Fe-doped gadolinium gallium

This article is part of the Topical Collection on *Proceedings of the International Conference on the Applications of the Mössbauer Effect (ICAME 2015), Hamburg, Germany, 13–18 September 2015*

✉ H. P. Gunnlaugsson
haraldur.p.gunnlaugsson@cern.ch

¹ Institute for Nuclear Research and Nuclear Energy, Bulgarian Academy of Sciences, 72 Tsarigradsko Chaussee Boulevard, Sofia, 1784, Bulgaria

² CERN, PH Div, CH-1211 Geneve 23, Switzerland

³ Tokyo University of Science, Tokyo, Japan

⁴ Physics and Engineering Department, University of Zululand, Zululand, South Africa

⁵ Department of Physics, K.N. Toosi University of Technology, P.O.Box 15875-4416, Tehran, Iran

⁶ School of Physics, University of the Witwatersrand, Witwatersrand 2050, South Africa

⁷ Laboratorio MDM, IMM-CNR, Via Olivetti 2, I-20864 Agrate Brianza (MB), Italy

⁸ Moscow Institute of Physics and Technology, 9 Institutskiy per., Dolgoprudny, Moscow Region, 141700, Russian Federation

⁹ BCMaterials & Elektrizitate eta Elektronika Saila, Euskal Herriko Unibertsitatea (UPV/EHU), 48048 Bilbao, Spain

garnet $\text{Gd}_3\text{Ga}_5\text{O}_{12}$ (GGG), with implantation fluences between 8×10^{15} and 6×10^{16} atoms cm^{-2} . Three Fe components are observed in the emission Mössbauer spectra: (i) high spin Fe^{2+} located at damage sites due to the implantation process, (ii) high spin Fe^{3+} at substitutional tetrahedral Ga sites, and (iii) interstitial Fe, probably due to the recoil imparted on the daughter ^{57}Fe nucleus in the β^- decay of ^{57}Mn . In contrast to high fluence ^{57}Fe implantation studies the Fe^{3+} ions are found to prefer the tetrahedral Ga site over the octahedral Ga site. No annealing stages are evident in the temperature range investigated. Despite the very low concentration, high-spin Fe^{3+} shows fast spin relaxation, presumably due to an indirect interaction between nearby gadolinium atoms.

Keywords Gadolinium gallium garnet ($\text{Gd}_3\text{Ga}_5\text{O}_{12}$) · ^{57}Mn implantation · Mössbauer emission spectroscopy · Fe sites

1 Introduction

Iron doping of gadolinium gallium garnet $\text{Gd}_3\text{Ga}_5\text{O}_{12}$ (GGG) has been shown to enhance the magnetocaloric effects of the material [1, 2]. It has been suggested that this is due to Fe^{3+} ions mediating exchange interactions between Gd ions, but no microscopic investigation of this effect has been performed. In this study we investigate the Fe doping by ion-implantation in the truly dilute ($< 10^{-4}$ at%) regime utilising ^{57}Fe emission Mössbauer spectroscopy (eMS).

The cubic structure of the gadolinium gallium garnet is illustrated in Fig. 1. It is formed as $[\text{C}]_3([\text{A}]_2[\text{D}]_3)\text{O}_{12}$ with a unit cell comprising eight sublattices. Gd ions as [C] ions are located at dodecahedral (24c) sites, while Ga ions as [A] and [D] ions occupy octahedral (16a) and tetrahedral (24d) sites, respectively.

Earlier Mössbauer Spectroscopy study of Fe-doped GGG [4], with implantation fluences between 8×10^{15} to 6×10^{16} atoms cm^{-2} and after annealing up to 600°C , found the implanted Fe^{3+} substituted gallium atoms both at the octahedral and the tetrahedral positions, with the octahedral site preferred at the highest fluences. Fe^{3+} in the octahedral site was characterized by an isomer shift of $\delta = 0.35$ mm/s and a quadrupole splitting of $\Delta E_Q = 0.37$ mm/s and the corresponding parameters in the tetrahedral site were $\delta = 0.16$ mm/s and $\Delta E_Q = 1.03$ mm/s.

2 Experimental

Radioactive beams of $^{57}\text{Mn}^+$ ($T_{1/2} = 85.4$ s) were produced at the ISOLDE facility at CERN by 1.4 GeV proton-induced fission in a heated UC_2 target and elemental selective laser multi-photon ionization [5]. After acceleration to 50 keV and magnetic mass separation, pure beams of $\sim 2 \times 10^8$ $^{57}\text{Mn}^+$ /s were obtained.

¹⁰ Physics Department, Durban University of Technology, Durban 4000, South Africa

¹¹ Science Institute, University of Iceland, Dunhaga 3, IS-107 Reykjavík, Iceland

¹² Instituut voor Kern- en Stralingsfysika, University of Leuven, B-3001 Leuven, Belgium

¹³ School of Chemistry and Physics, University of KwaZulu-Natal, Durban 4000, South Africa

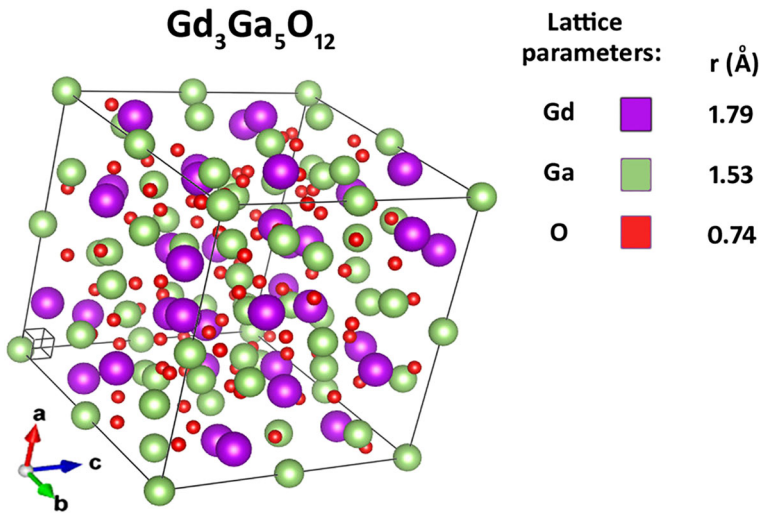


Fig. 1 Lattice structure of Gd₃Ga₅O₁₂ garnet showing the distribution of the Gd, Ga and O ions [3]

Dilute ⁵⁷Mn⁺ ions were implanted into Gd₃Ga₅O₁₂ single crystal samples at an incident angle of $\theta_1 = 30^\circ$ relative to the sample surface normal. Emission Mössbauer spectra (eMS) were measured on-line on the 14.4 keV Mössbauer state of the daughter ^{57*}Fe ($T_{1/2} = 98$ ns) with an acetone gas-filled parallel-plate avalanche resonance detector, equipped with stainless steel electrode enriched in ⁵⁷Fe. The experimental line-width of the detector and setup is described with a Voigt profile with Lorentzian FWHM broadening of $\Gamma_D = 0.34$ mm/s and Gaussian broadening of $\sigma_D = 0.08$ mm/s. The detector was mounted outside the implantation chamber on a conventional constant-acceleration drive system at 90° relative to the beam direction (60° relative to the normal to the crystal surface). The spectra were recorded continuously for 10 min. from the start of the implantation. The maximum implanted fluence was ($\sim 2 \times 10^{12}$ ⁵⁷Mn/cm²) corresponding to a local concentration of less than 10^{-4} at.%. The samples were measured and held at the different temperatures by a lamp heating the sample backside. Velocities and isomer shifts are given relative to the centre of the α -Fe spectrum at room temperature.

3 Results

The ⁵⁷Fe eMS obtained after implantation of ⁵⁷Mn into a Gd₃Ga₅O₁₂ single crystal at sample temperatures between 303 K and 563 K, are presented in Fig. 2.

The overall shape of the spectra is a convolution of two or more doublets with no sign of any magnetically-split sextet component. A fitting strategy was adopted in which three doublet components with Voigt line-shapes were applied (Fig. 2) to simultaneously fit the spectra over the entire temperature range of measurements, assuming temperature independent line-widths. The resulting hyperfine parameters are gathered in Fig. 2, with corresponding site assignments as discussed below and the relative areas in Fig. 3.

The isomer shift data for all three doublets followed the second order Doppler (SOD) shift with temperature. The broad lines associated with DB1 suggest Fe in highly distorted

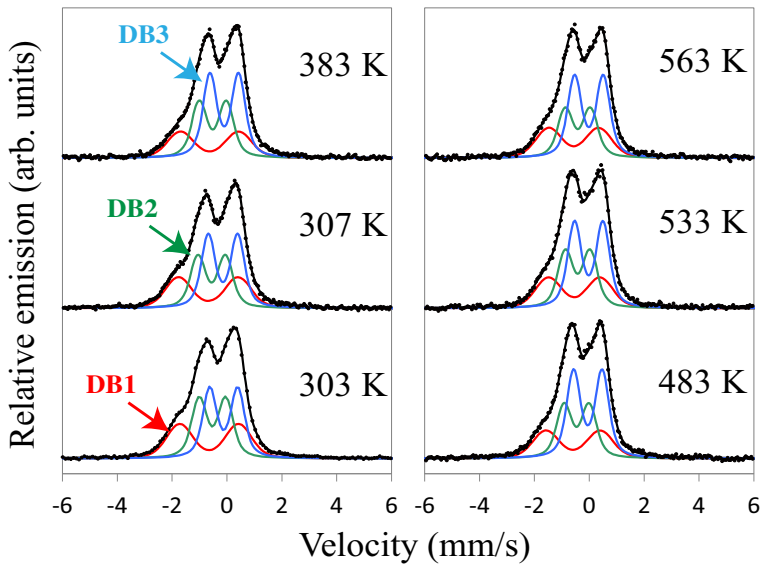


Fig. 2 ^{57}Fe eMS spectra obtained after implantation of ^{57}Mn into GGG crystals held at the temperatures indicated. The solid lines show the fitting components as labelled and their sum

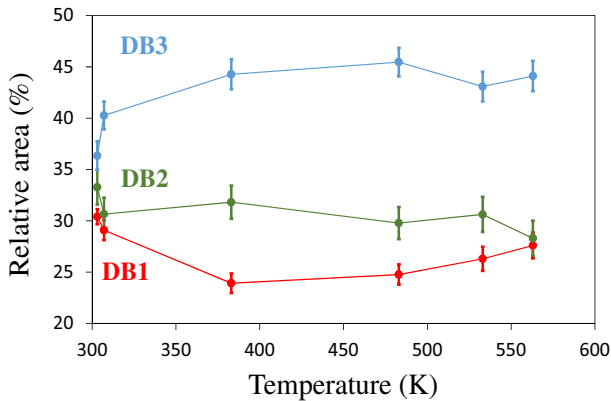


Fig. 3 Relative areas of the spectral components as a function of temperature

lattice environment, due to extended lattice damage resulting from the implantation process. The hyperfine parameters are consistent with high-spin Fe^{2+} in amorphous zones as observed in several ion implanted insulators [6].

4 Discussion

The isomer shift and negligible temperature dependence of the quadrupole splitting (Table 1) of DB3 are consistent with an assignment as originating from high-spin Fe^{3+} . In order to interpret this component further, we discuss it in comparison with results

Table 1 Summary of hyperfine parameters. δ_{RT} is the isomer shift at room temperature, $\Delta E_{Q,RT}$ the quadrupole splitting at room temperature, $d\Delta E_Q/dT$ the temperature dependence of the quadrupole splitting throughout the temperature range and σ the Gaussian broadening of the spectral lines additional to the experimental line width of the detector

Component	Site assignment	δ_{RT} (mm/s)	$\Delta E_{Q,RT}$ (mm/s)	$d\Delta E_Q/dT$ (mm/(s.K))	σ (mm/s)
DB1	Fe ²⁺ damage	0.65(1)	2.15(4)	-120(20)×10 ⁻⁵	0.33(1)
DB2	Interstitial Fe	0.53(1)	0.97(1)	-34(5)×10 ⁻⁵	0.19(1)
DB3	Fe ³⁺ on Ga _T sites	0.12(1)	1.02(1)	-3(4)×10 ⁻⁵	0.17(1)

obtained on ⁵⁷Fe implanted samples in the fluence range from 8×10¹⁵ – 6×10¹⁶ cm⁻² of Szucs et al., [4]. Their spectra, after annealing at $T \geq 600^\circ\text{C}$, showed three components: “Prec” assigned to Fe in Fe³⁺ containing precipitates, “T” assigned to Fe³⁺ on tetrahedral Ga sites and “O” assigned to Fe³⁺ on octahedral Ga sites [4]. The hyperfine parameters of the “T” component ($\delta_{RT} = 0.16$ mm/s, $\Delta E_{Q,RT} = 1.03$ mm/s) correspond well with the DB3 component observed here (see Table 1). The temperature dependence of the quadrupole splitting of the DB3 component likewise supports this identification, since it exhibits an insignificant variation (see Table 1), as is expected for high-spin Fe³⁺.

DB2 is characterized by a relatively small line-width suggesting a more regular crystalline site (not amorphous site). The hyperfine parameters of DB2 in our study are different from the components observed in higher fluence ⁵⁷Fe implanted samples [4], in particular, the isomer shift observed here ($\delta_{RT} = 0.53(1)$ mm/s) is inconsistent with Fe³⁺ on octahedral Ga sites ($\delta_{RT} = 0.35$ mm/s [4]). A tentative assignment of DB2 could therefore be interstitial Fe, either due to implantation directly on interstitial sites or due to the recoil ($\langle E_R \rangle = 40$ eV, $E_{R,Max} = 93$ eV) imparted on the ⁵⁷Fe daughter nucleus in the β^- decay of ⁵⁷Mn resulting in a relocation of the Fe to interstitial sites. In comparison, the calculated threshold displacement energy for Gd₃Ga₅O₁₂ has been estimated as ~ 56 eV [7], far less than the maximum recoil energy and the assignment of the DB2 originating from interstitial Fe is the most likely. From the present experimental data it is not possible to determine the ionic state of the interstitial Fe.

In the super-dilute regime reported here, we thus observe that the implanted Fe³⁺ is found to occupy only tetrahedral Ga sites and there is no evidence of octahedral substitution. This contrasts the observations of Szucs et al. [4], where the octahedral occupancy could be a consequence of the relatively high iron concentration.

It is of interest to note, that despite the extreme dilution used, sextet-like spectral components due to slow paramagnetic relaxation of Fe³⁺ are not observed as in similar eMS experiments in other oxides [8–11]. Instead high-spin Fe³⁺ (Fe³⁺ on Ga_T sites, DB3) show fast ($> 10^{10}$ Hz) spin relaxation and is observed as a doublet. This indicate that there is an interaction between Fe and Gd ions which would result in fast spin-spin relaxations. This is in agreement with the observation of McMichael et al., [12] who observed enhanced magnetocaloric effect proposed to originate from Fe³⁺ mediating exchange interaction between Gd³⁺ ions.

Within the temperature range of this study, definite signs of an annealing stage are not observed which, for example, would be noted as a prompt change in the area fractions (Fig. 3), suggesting that annealing at higher temperature is needed to incorporate all ions on regular lattice sites.

5 Conclusion

We have by means of emission Mössbauer spectroscopy investigated the lattice sites occupied of dilute Fe in $\text{Gd}_3\text{Ga}_5\text{O}_{12}$ in the temperature range from room temperature to 563 K. Dilute ion-implantation results in three components; high spin Fe^{3+} on substitutional Ga_T sites, interstitial Fe, and Fe^{2+} in amorphous zones. No annealing stage between RT and ~ 560 K is observed. High spin Fe^{3+} in this material shows fast spin relaxation despite the very low concentration ($<10^{-4}$ at.%) utilized in this study, presumably due to exchange interaction with Gd^{3+} .

Acknowledgments This work was supported by the European Union Seventh Framework through ENSAR (Contract No. 262010). R. Mantovan acknowledges support from MIUR through the FIRB Project RBAP115AYN “Oxides at the nanoscale: multifunctionality and applications.” V. Adoons, K. Bharuth-Ram, H. Masenda, D. Naidoo, and M. Ncube acknowledge support from the South African National Research Foundation and the Department of Science and Technology. T. E. Møllholt, H. P. Gislason, and S. Ólafsson acknowledge support from the Icelandic Research Fund (Grant No. 110017021-23). I. Unzueta acknowledges financial support from Basque Government Grants nos. IT-443-10 and PRE_2014_214.

References

1. Provenzano, V., Li, J., King, T., Canavan, E., Shirron, P., DiPirro, M., Shull, R.D.: Enhanced magnetocaloric effects in $\text{R}_3(\text{Ga}_{1-x}\text{Fe}_x)_5\text{O}_{12}$ ($\text{R}=\text{Gd, Dy, Ho}$; $0 < x < 1$) nanocomposites. *J. Magn. Magn. Mater* **266**, 185–193 (2003). doi:[10.1016/S0304-8853\(03\)00470-0](https://doi.org/10.1016/S0304-8853(03)00470-0)
2. Matsumoto, K., Matsuzakiy, A., Kamiya, K., Numazawa, T.: Magnetocaloric effect, specific heat, and entropy of iron-substituted Gadolinium Gallium Garnets $\text{Gd}_3(\text{Ga}_{1-x}\text{Fe}_x)_5\text{O}_{12}$. *Jpn. J. Appl. Phys* **48**, 113002 (2009). doi:[10.1143/JJAP.48.113002](https://doi.org/10.1143/JJAP.48.113002)
3. Momma, K., Izumi, F.: VESTA 3 For three-dimensional visualization of crystal, volumetric and morphology data. *J. Appl. Crystallogr.* **44**, 1272–1276 (2011). doi:[10.1107/S0021889811038970](https://doi.org/10.1107/S0021889811038970)
4. Szucs, I., Dezsi, I., Fetzter, Cs., Langouche, G.: Iron implantation in gadolinium gallium garnet studied by conversion-electron Mössbauer spectroscopy. *J. Phys. Condens Mat* **10**, 101–110 (1998). doi:[10.1088/0953-8984/10/1/012](https://doi.org/10.1088/0953-8984/10/1/012)
5. Fedoseyev, V.N., Bätzner, K., Catherall, R., Evensen, A.H.M., Forkel-Wirth, D., Jonsson, O.C., Kugler, E., Lettry, J., Mishin, V.L., Ravn, H.L., Weyer, G., ISOLDE Collaboration: Chemically selective laser ion source of manganese. *Nucl. Instr. Meth. B* **126**, 88–91 (1997). doi:[10.1016/S0168-583X\(96\)01077-4](https://doi.org/10.1016/S0168-583X(96)01077-4)
6. Dezsi, I., Coussement, R., Feher, S., Langouche, G., Fetzter, Cs.: The charge states of iron in insulators implanted with ^{57}Co and ^{57}Fe . *Hyperfine Interact.* **29**, 1275–1278 (1986). doi:[10.1007/BF02399467](https://doi.org/10.1007/BF02399467)
7. Ubizskii, S.B., Matkovskii, A.O., Mironova-Ulmane, N., Skvortsova, V., Suchocki, A., Zhydachevskii, Y.A., Potera, P.: Displacement Defect Formation in Complex Oxide Crystals. *Phys. Stat. Sol. (a)* **177**, 349–366 (2000). doi:[10.1002/\(SICI\)1521-396X\(200002\)177:2349::AID-PSSA3493.0.CO;2-B](https://doi.org/10.1002/(SICI)1521-396X(200002)177:2349::AID-PSSA3493.0.CO;2-B)
8. Gunnlaugsson, H.P., Møllholt, T.E., Mantovan, R., Masenda, H., Naidoo, D., Dlamini, W.B., Sielemann, R., Bharuth-Ram, K., Weyer, G., Johnston, K., Langouche, G., Ólafsson, S., Gislason, H.P., Kobayashi, Y., Yoshida, Y., Fanciulli, M., the ISOLDE Collaboration: Paramagnetism in Mn/Fe implanted ZnO. *Appl. Phys. Lett.* **97**, 142501 (2010). doi:[10.1063/1.3490708](https://doi.org/10.1063/1.3490708)
9. Gunnlaugsson, H.P., Mantovan, R., Møllholt, T.E., Naidoo, D., Johnston, K., Masenda, H., Bharuth-Ram, K., Langouche, G., Ólafsson, S., Sielemann, R., Weyer, G., Kobayashi, Y., the ISOLDE collaboration: Mössbauer spectroscopy of ^{57}Fe in $-\text{Al}_2\text{O}_3$ following implantation of ^{57}Mn . *Hyperfine Interact.* **198**, 5–13 (2010). doi:[10.1007/s10751-010-0184-5](https://doi.org/10.1007/s10751-010-0184-5)
10. Mantovan, R., Gunnlaugsson, H.P., Johnston, K., Masenda, H., Møllholt, T.E., Naidoo, D., Ncube, M., Shayestehaminzadeh, S., Bharuth-Ram, K., Fanciulli, M., Gislason, H.P., Langouche, G., Ólafsson, S., Pereira, L.M.C., Wahl, U., Torelli, P., Weyer, G.: Atomic-scale magnetic properties of truly 3d-diluted ZnO. *Adv. Electron. Mater* **1**, 1400039 (2015). doi:[10.1002/aelm.201400039](https://doi.org/10.1002/aelm.201400039)
11. Møllholt, T.E., Gunnlaugsson, H.P., Johnston, K., Mantovan, R., Masenda, H., Ólafsson, S., Bharuth-Ram, K., Gislason, H.P., Langouche, G., Weyer, G., the ISOLDE Collaboration: Spin-lattice relaxations of paramagnetic Fe_3^+ in ZnO. *Phys. Scripta* **T148**, 014006 (2012). doi:[10.1088/0031-8949/2012/T148/014006](https://doi.org/10.1088/0031-8949/2012/T148/014006)
12. McMichael, R.D., Ritter, J.J., Shull, R.D.: Enhanced magnetocaloric effect in $\text{Gd}_3\text{Ga}_5\text{Fe}_x\text{O}_{12}$. *J. Appl. Phys* **73**, 6946 (1993). doi:[10.1063/1.352443](https://doi.org/10.1063/1.352443)